

Top Surface Imaging at 157 nm

Andrew Jamieson^a, Mark Somervell^b, Hoang Vi Tran^a, Raymond Hung^a, Scott A. MacDonald^c,
C. Grant Willson^a

^a Department of Chemical Engineering, The University of Texas at Austin, Austin, TX 78712

^b Currently at Texas Instruments, Dallas, TX, 75243

^c IBM Almaden Research Center, San Jose, CA 95129

ABSTRACT

Top surface imaging (TSI) has had an interesting history. This process showed great promise in the late 1980's and several attempts were made to introduce it to full-scale manufacturing. Unfortunately, defect density problems limited the process and it fell from favor. TSI emerged again as an important part of the EUV and 193 nm strategies in the early stages of those programs because it offered a solution to the high opacity of common resist materials at both wavelengths. A flurry of research in both areas identified the seemingly insurmountable problem of line edge roughness, which caused the process to be dropped from both programs. Recent developments in TSI have demonstrated the ability to print high-resolution, high-aspect ratio images at 193 nm with less line edge roughness than typical single layer resist systems. This has largely been due to the development of polymers specifically tailored for this end use. The optimum materials must be moderately transparent and have high Tg's in the silylated state. The 157 nm program has much in common with the early stages of the 193 nm program. The optical density of even 193 nm resist materials at 157 nm is far too high to allow their use in single layer applications. The less stringent optical density requirements of TSI make it a potentially viable imaging scheme for use at 157 nm. Various TSI materials, including the traditional poly (*t*-BOC-hydroxystyrene), as well as novel aliphatic cyclic polymers bearing bis-trifluoromethyl carbinol substituents, have been investigated for use at 157 nm, and smooth high-resolution images have been generated.

1. INTRODUCTION

The semiconductor industry continues to drive toward production of devices with smaller and smaller critical dimensions. This quest has generated many difficult challenges. When the industry moved to 248 nm exposure light, the challenge was to find a material that was appropriately transparent and which functioned with low energy doses. Chemical amplification with poly-hydroxystyrene based systems overcame these obstacles. At 193 nm, the primary challenge lay in optical transparency, since phenolic materials absorbed strongly. Fortunately, it was found that alicyclic materials such as norbornene and adamantane provided both transparency and the requisite etch resistance.

Today, at the wavelength of 157 nm, the industry faces the same optical density challenge, but with a much more limited set of transparent functional groups from which to work. At 157 nm, nearly everything absorbs light, including the C-C bond. Preliminary work by Kunz¹ and others² indicates that polymer systems based on siloxanes and fluoro-carbons are the most transparent platforms for resist design, and functional, etch resistant photoresists have now been formulated with absorbances of less than $3 \mu\text{m}^{-1}$ ³. However, even with polymer systems that are this transparent, in order to achieve appropriate sidewall angles, resist coatings will have to be fairly thin, usually less than 200 nm. This thickness is not adequate for many subsequent etch processes, and in case absorbance does not drop to adequate levels for single layer systems, many people are looking into alternative imaging schemes including inorganic BARC "hardmasks"^{4,5}, bi-layer processes⁶ and top surface imaging⁷. Further motivating the push towards alternative imaging schemes is the problem of feature collapse in base-developed systems. Studies by researchers at University of Wisconsin and International SEMATECH show that the critical aspect ratio of collapse scales roughly linearly with pitch, and as such, 70 nm nested lines will likely be limited to aspect ratios of less than 2 in wet developed systems⁸.

This paper focuses on the application of top surface imaging to 157 nm. The TSI systems studied in this paper are ones in which the silylation contrast is created by a photo-induced switch in the chemical reactivity of the polymer. A polymer that

2. EXPERIMENTAL AND MATERIALS

2.1 Materials

Poly (*t*-BOC-Styrene) (*t*-BOCPS) was prepared by polymerization of 4-*t*-butyloxycarbonyloxystyrene monomer donated by Triquest chemical company. A typical polymerization procedure is given below. *t*-BOC-styrene monomer, (20g, 0.091 mol), was dissolved in dry THF (40mL) in a round bottom flask. The solution was heated to 60°C and then 0.2g of AIBN (0.2g) was added. The resulting solution was stirred overnight, cooled to room temperature, and diluted with an additional 20ml of THF. The THF solution was added to 1L of rapidly stirred methanol whereupon a white precipitate formed. The polymer was isolated by filtration, dried *in vacuo* at room temperature for 24 hours, redissolved in THF, and then reprecipitated. The resulting white polymer powder was obtained in 85% yield after the two precipitations and typically had a number averaged molecular weight of 25,000 with a M_w / M_n of 1.8.

Poly (*t*-BOC-norbornyl hexafluoro alcohol alt-SO₂) (PFASO₂) was prepared by the free radical polymerization of SO₂ with *t*-BOC-hexafluoroalcoholnorbornene. A typical polymerization procedure is given below. Sulfur dioxide (25mL) was condensed in a round bottom flask at -41°C (dry ice / acetonitrile). A solution of *t*-BOC-hexafluoroalcoholnorbornene (5g, 13.3 mmol) in 22.5 ml dry THF was added. A solution of *t*-butylhydroperoxide (23μl, 0.31 mmol) was added in 2 ml dry THF, and the reaction vessel was stirred for 4 hours. In order to quench the reaction, hydroquinone (70mg, 0.64 mmol) was added, and the flask was allowed to warm to room temperature after the polymerization, evolving SO₂ gas. The polymer solution was mixed with 75ml of ethyl acetate and washed with 5% NaHCO₃ in water until neutral. The organic phase was then washed with water (3x) and with brine (2x), and dried with MgSO₄. Ethyl acetate was evaporated, and the polymer was redissolved into a minimum volume of THF. The polymer was precipitated into hexane, filtered, and dried *in vacuo* at room temperature overnight (3.0g, 51%).

Poly (*t*-BOC- norbornyl hexafluoro alcohol) (PNFA) was synthesized by *t*-BOC protection of poly (NB-HFOH) with di-*tert*-butyl dicarbonate. Poly (NB-HFOH) was prepared by Pd²⁺ catalyzed addition polymerization in dichloromethane at room temperature, as described in Hung *et al*⁴. Poly(NB-HFOH) (3.13 g, 11.4 mmol) and di-*tert*-butyl dicarbonate (5.4 g, 22.8 mmol) were dissolved in 40 ml THF. The solution was stirred at room temperature for 5 minutes. 4-(dimethylamino) pyridine (0.21 g, 1.14 mmol) was added to the reaction solution. The reaction was stirred overnight at room temperature. The polymer was precipitated into methanol (500 ml), filtered, and dried *in vacuo* at 50°C to give a white powder (3.2 g).

Dimethylaminodimethylsilane (DMADMS) was purchased from Silar Laboratories, and 1,2-dimethylaminodimethyldisilane (DMADMDS) was donated to us by Dr. David Wheeler from Sandia National Laboratories. DMADMDS was used in imaging and contrast curve experiments, while DMADMS was used in the FTIR experiments with PNFA for proof of silylation.

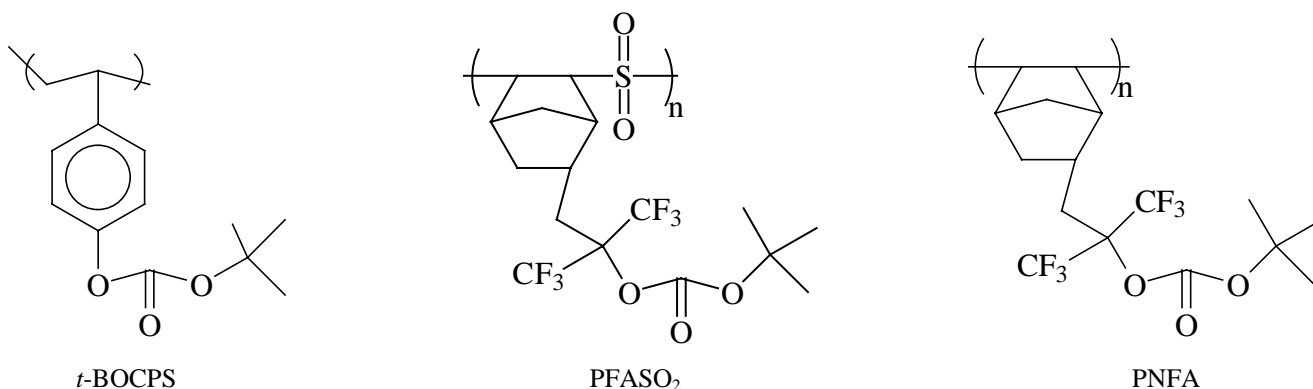


Figure 2. The three polymer systems used in this study.

2.2 Experimental Apparatus

Wafers were coated and baked using an FSI Polaris 2000 track. All 157 nm exposures were done using an Exitech micro-stepper at International SEMATECH (NA = 0.6). For binary mask exposures, $\sigma = 0.7$, for alternating aperture phase-shifted exposures, $\sigma = 0.3$. Silylation was performed using a Genesis 200C at 90°C with DMADMS for varying times and pressures that are described for each polymer system. Etching was performed on a LAM 9400 SE with the following settings: top power = 260 watts, bottom power 75 watts, pressure = ~3.2 mTorr O₂, flowrate 60sccm O₂, and bottom chuck T = -25°C. Endpoint detection for imaging was done using Endpoint Plus with 30% over-etch. Thickness was measured using a Prometrix interferometer using cauchy coefficients obtained for each polymer system using a Woolham VASE ellipsometer. SEM work was done using a Joel tilt SEM and a Hitachi 4500. Absorbance data was taken with a Woolham VUV VASE ellipsometer. IR spectra were taken on-wafer using a Nicolet Magna FTIR 550. For the contrast curve experiments, pad exposures were performed at 248 nm using an Ultratech XLS stepper.

3. RESULTS AND DISCUSSION

3.1 Imaging Experiments

3.1.1 Top Surface Imaging of *t*-BOCPS

Previous work⁷ with *t*-BOCPS at 193 nm indicated that line edge roughness was largely due to two factors. The first factor is the high opacity of *t*-BOCPS at 193 nm. The high opacity results in poor feature edge definition, and a stochastic etch mask degradation process along the edge of the feature during the etch step. The second factor is the low T_g of the silylated form of the polymer of 70°C. The silylation reaction is run at a temperature of 90°C, and as such, during the silylation step, the polymer is mobile, and the image can blur as a result of flow, phase separation or some other mechanism. For this work at 157 nm, the transparency of the resist is significantly better than at 193 nm (as can be seen in Fig. 3), which is expected to improve imaging performance. This is a necessary, but not sufficient characteristic. The low T_g of the silylated polymer should still result in roughness.

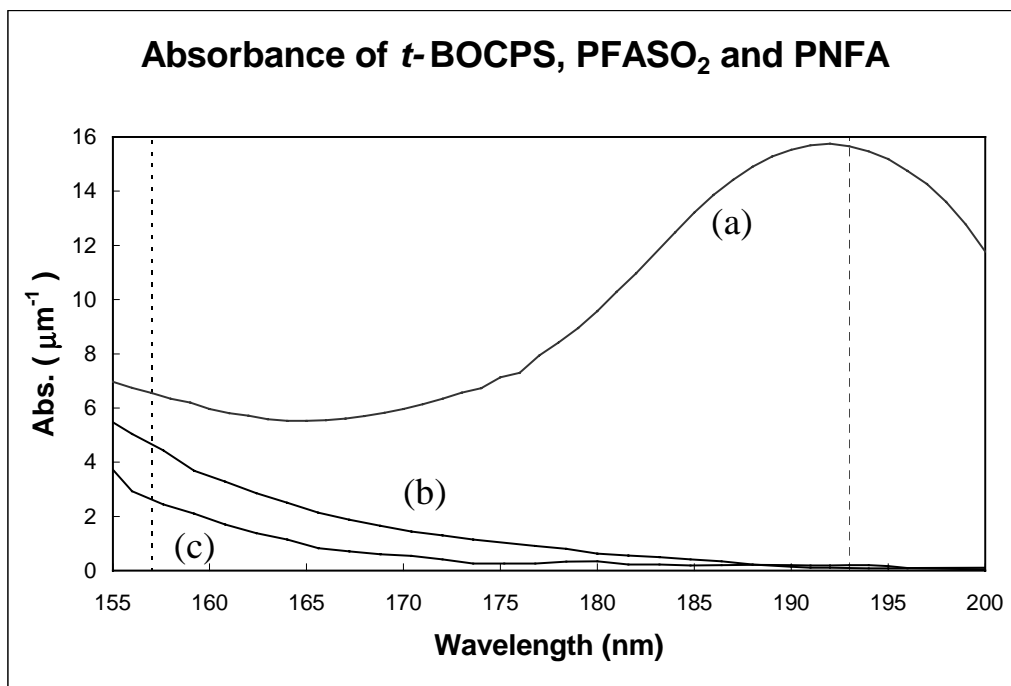


Figure 3. Absorbance (a) *t*-BOCPS, (b) PFASO₂, and (c) PNFA as a function of wavelength

t-BOCPS was formulated with 4% DPI-Nf (wt PAG / wt Poly) and 5% trioctylamine (moles base / moles PAG) in PGMEA. PAB was 100°C for 60s, PEB 100° for 60s. The resist was silylated at 90°C for 60s at 30 torr DMADMDs. The resist was imaged at 157 nm using a binary mask and the resulting images are shown in Fig. 4.

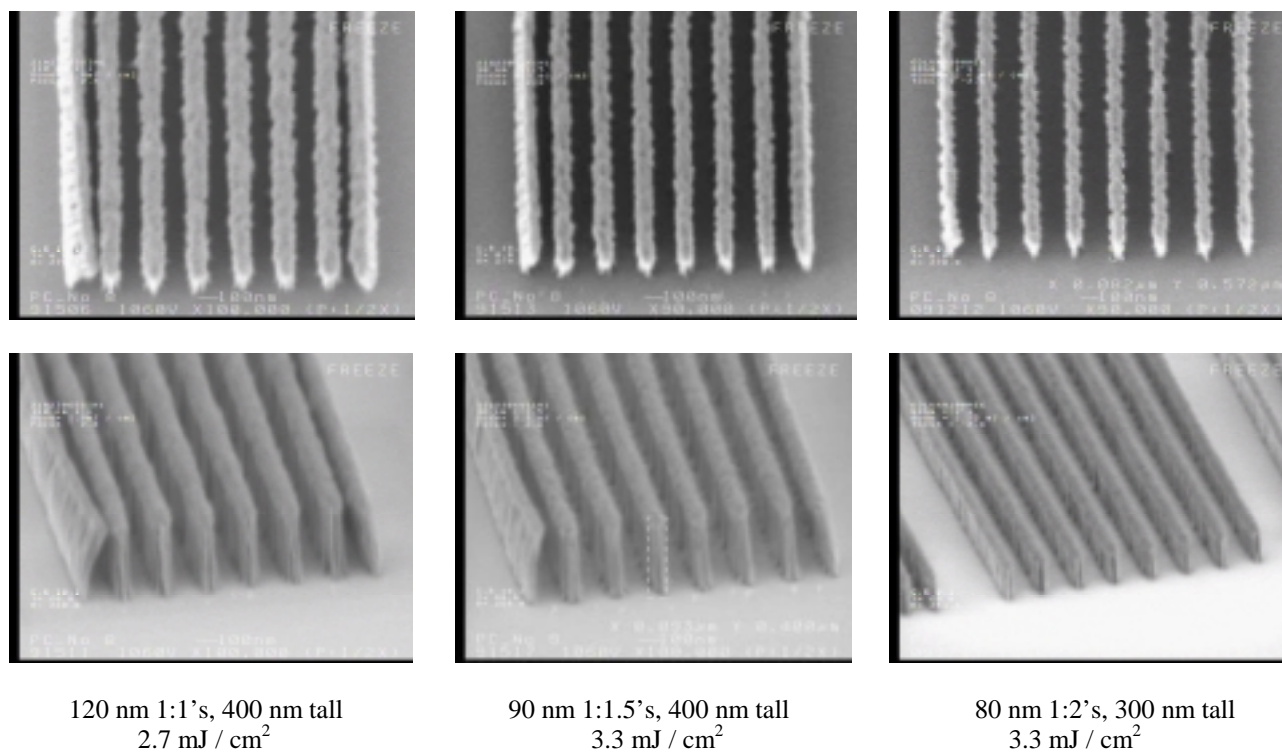


Figure 4. Top down and Tilted SEM of *t*-BOCPS imaged with a binary mask at 157 nm.

This resist prints with rough sidewalls, but the aspect ratio is extremely high, and the resolution is near the limit of the tool with a binary mask.

3.1.2 Top Surface Imaging of PFASO₂

Previous work⁷ with PFASO₂ at 193 nm showed the ability to print high-resolution, high-aspect ratio images with extremely low Line Edge Roughness (LER). The extremely low LER of this system was attributed to two advantageous material properties: low opacity and a high T_g of the silylated polymer (~105°C). At 157 nm the opacity of the resist is higher, as can be seen in Fig. 3, and as such, the effects of the wavelength change are unclear. Fortunately though, the glass transition temperature is above the temperature of the silylation step.

PFASO₂ was formulated with 4% TPS-Nf (wt PAG / wt Poly) and 10% trioctylamine (moles base / moles PAG). PAB and PEB were both run at 90°C for 60s. The resist was silylated at 90°C for 300s at 40 torr DMADMDs. The resist was imaged at 157 nm using a binary mask and the resulting images are shown in Fig. 5.

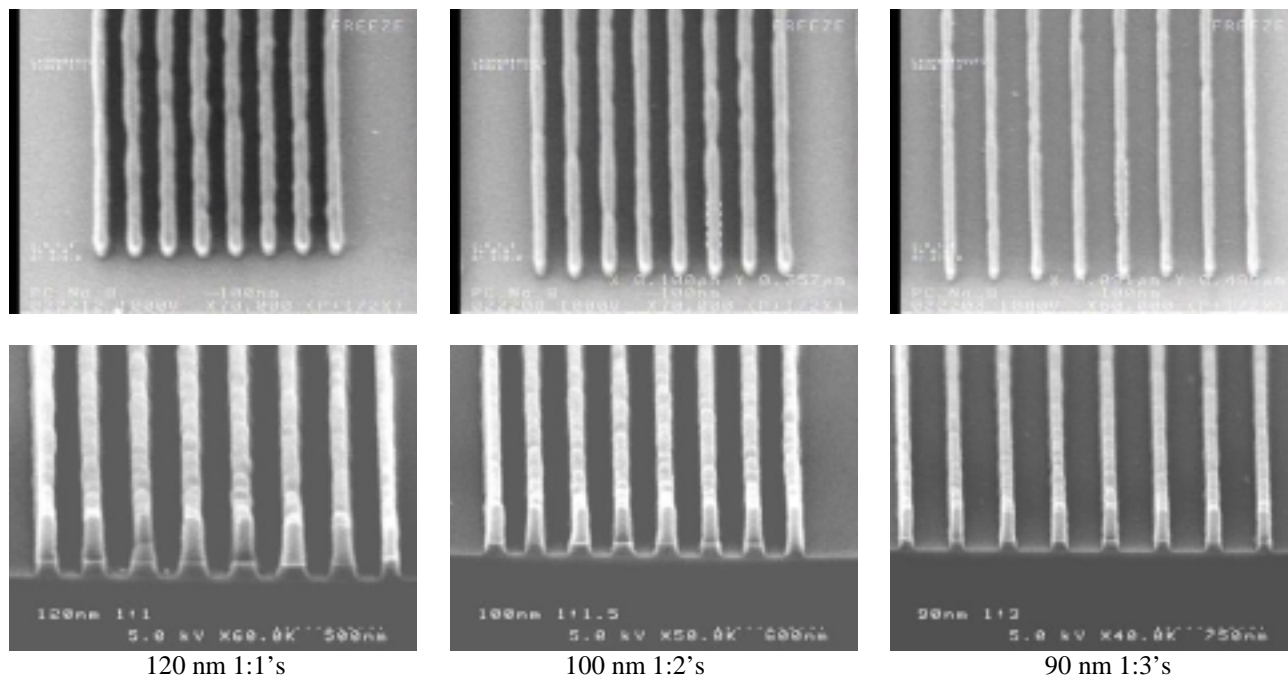


Figure 5. Top down and Tilted SEMs of PFASO₂ imaged at 157 nm with a binary mask. All features are 270 nm tall

The imaging quality is excellent and the edges are relatively smooth. The images show some low-frequency LER, but the high-frequency roughness that is characteristic of most TSI systems is not present. The dose required to print these images is between 80- 110 mJ / cm². The process hasn't been optimized, (in fact these images were taken from the second wafer we processed at high doses), and it is likely that with optimization of the bake temperatures and etch conditions, the low-frequency roughness can be overcome. Overall, these images show that printing smooth lines with TSI at 157 nm is possible.

3.1.3 Top Surface Imaging of PNFA

PNFA is a material that was generated as a byproduct of our 157 nm single-layer resist program. It has promising material properties in that it has high silicon content after silylation (15.5% wt), is more transparent than PFASO₂, (see Fig. 3), and is expected to have a high Tg in its silylated state. (We are in the process of determining the Tg of the silylated form of this compound.)

In order to insure that PNFA deprotected and silylated properly, we first studied the silylation of the material with IR. PNFA was formulated with 6% TPS-Nf (wt PAG / wt Poly) and 10% trioctylamine (moles base / moles PAG). The resist was coated, baked, flood exposed at 248 nm, and silylated. PAB and PEB were both run for 60s at 130°C. Silylation was at 90°C for 120s with 40torr DMADMS. The infrared spectrum of PNFA was collected after the PAB, after the PEB, and after silylation. The resulting spectra are shown in Fig. 6. The complete disappearance of the carbonyl peak at ~1770 cm⁻¹ coupled with the appearance of the OH peak at ~3500 cm⁻¹ after exposure indicates complete deprotection, and the appearance of the Si-H peak at ~2100 cm⁻¹ in the silylated spectra accompanied by the complete disappearance of the OH peak at ~3500 cm⁻¹ indicates complete silylation. Analogous spectra of *t*-BOCPS and PFAS have been published previously^{7,12}).

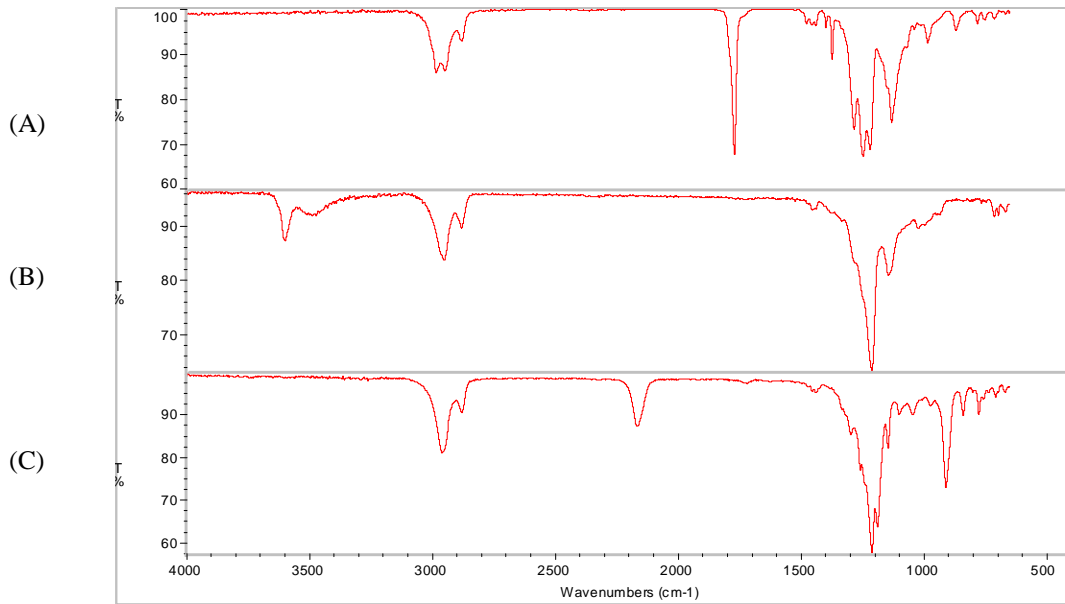


Figure 6. Infrared Spectra of PNFA (a) after coating, (b) after exposure and PEB and (c) after silylation with DMADMS.

The resist was imaged at 157 nm using an alternating aperture phase-shifted mask and the resulting images are shown in Fig. 7. Process conditions were the same as described for the IR experiment, the only exception being the use of DMADMS instead of DMADMS. Unfortunately, the images printed with rough sidewalls. Imaging the resist at 193 nm, where the polymer is essentially completely transparent did not help. These results indicate that at some point in the process the film has been brought above the T_g of one of its components, most likely the silylated form of PNFA. This material has some, but not all of the attributes required for 157 nm TSI applications.

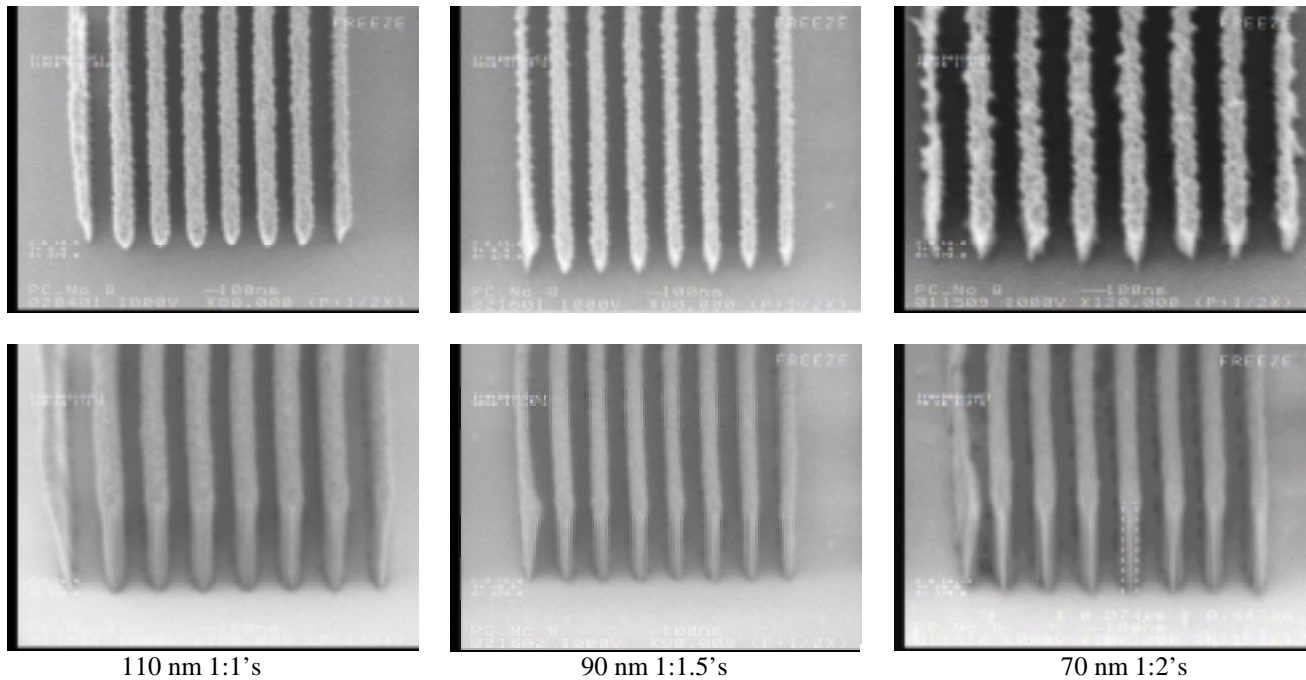


Figure 7. Top down and Tilted SEMs of PNFA imaged at 157 nm with a phase-shifted mask. All features 450 nm tall.

3.2 Contrast Curves

3.2.1 Generation of contrast curves

In order to gain a better understanding of the fundamental behavior of these TSI systems, contrast curves were generated through each step of the process by recording film thickness as a function of dose. It was verified that thickness changes correlate nearly exactly with changes in the chemical composition of the film by IR, by either monitoring the growth of the Si-H peak or by monitoring the loss of the carbonyl peak, (the thickness changes were not the result of density changes). Thickness was measured with an interferometer in each field of a 10 x 10 array after each of the following steps: PAB, PEB, silylation, 10s etch, 50s etch, and 110s etch. Flood exposures were performed at 248 nm where all three polymer systems are transparent. These curves are presented as Figs. 8, 9 and 10. Using an ellipsometer, it was found that the Cauchy coefficients varied little through deprotection and silylation, and as such, Cauchy coefficients for the protected compounds were used. All process conditions (formulation, PAB, PEB, silylation, etc) were the same as those used for imaging, with the exception of the *t*-BOCPS, where 2% TPS-Nf was used for contrast curves instead of 4% DPI-Nf.

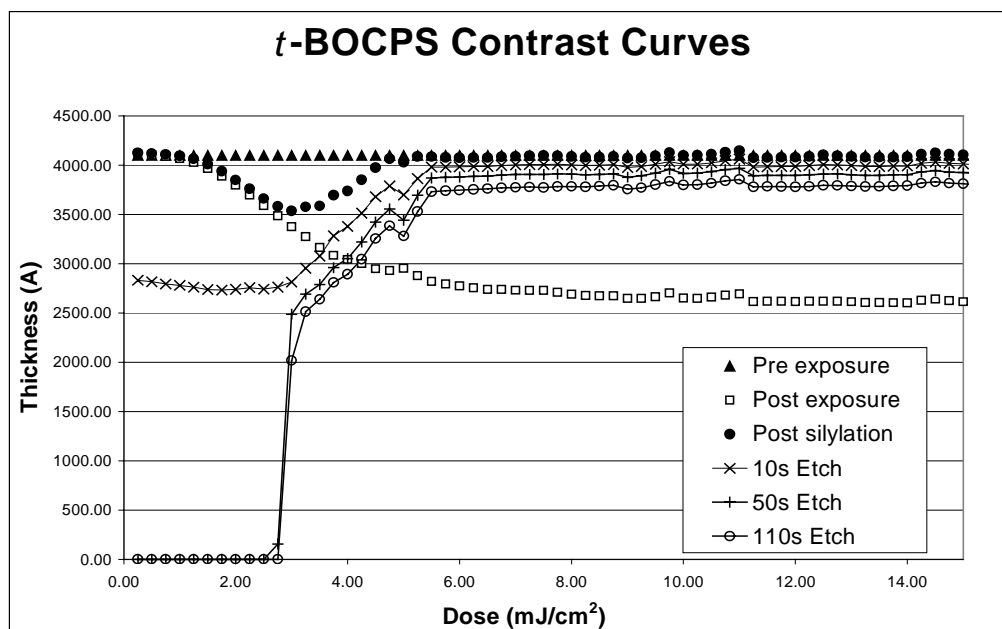


Figure 8. Contrast curves for *t*-BOCPS

3.2.2 Discussion of *t*-BOCPS contrast curve

These curves show a number of interesting aspects of this system. The chemical amplification step of this resist generates excellent contrast, as can be seen by the sharp thickness loss after exposure greater than $\sim 1 \text{ mJ} / \text{cm}^2$. The silylation of this resist also enhances the contrast of the system. Up until the resist is $\sim 50\%$ deprotected, the silylation agent does not permeate into the film (as can be seen by the lack of thickness increase upon silylation at doses of less than $\sim 3 \text{ mJ} / \text{cm}^2$). However, above 50% deprotection, the silylation agent readily permeates and reacts with the film. This is the only system that we have seen that exhibits this “silylation contrast” behavior. As is usually the case, *t*-BOCPS shows great contrast in its final etch step. The overall contrast in this system is excellent.

The very high silicon content of the silylated polymer (27%) results in an extremely low etch rate of the silylated resist. The blanket etch rate of the silylated resist after the silicon dioxide etch mask has been formed is $\sim 0.2 \text{ nm} / \text{s}$. The blanket etch

rate of the protected polymer is $\sim 13 \text{ nm / s}$. This excellent etch contrast enables the TSI system to function at wavelengths where the resist is nearly opaque since the light (and hence deprotection and silicon incorporation) does not need to go very deep into the film for an adequate etch barrier to be formed.

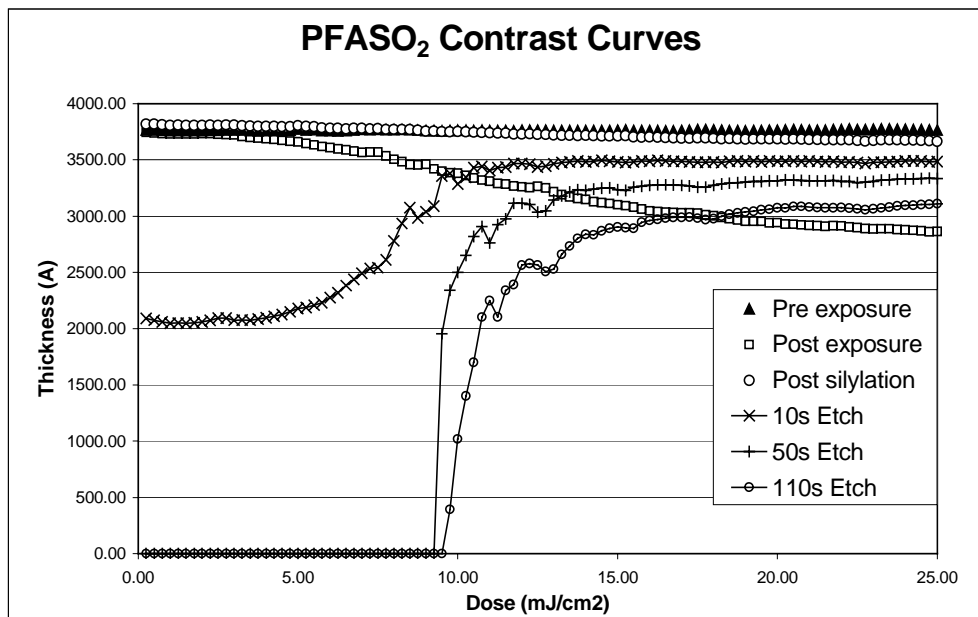


Figure 9. Contrast curves for PFASO₂

3.2.3 Discussion of contrast curves for PFASO₂

The contrast curves of the PFASO₂ system reveal a number of interesting aspects. First, the thickness curve after exposure and PEB shows that the deprotection step of this polymer is extremely slow. Typically, one would expect to see a much sharper transition, and this result is very puzzling. This curve was replicated by looking at the carbonyl peak in the IR across all the fields and by using a different batch of polymer that was neutralized after polymerization as described by Ito *et al*¹³. This poor deprotection contrast might be related to the relatively low PEB temperature of 90°C, but since the polymer begins to deprotect thermally at higher temperatures, it is not appropriate to run it at higher temperatures.

The post-silylation curve of this polymer indicates that no “silylation contrast” is present in the film, since the film fills back up to the initial thickness. Fortunately, the high etch contrast of system results in acceptable overall contrast in the system. The blanket etch rate of the silylated resist after the silicon dioxide etch mask has been formed of 0.4 nm/s is slightly higher in this system than in *t*-BOCPS. The blanket etch rate of the protected resist is 17 nm / s.

The higher etch rate of the silylated form of PFASO₂ likely plays a role in the high dose required for imaging at 157 nm. Due to the higher absorbance of this film, the energy deposition profile of the resist is much more shallow than was seen at 193 nm (where the dose to size was $\sim 15 \text{ mJ / cm}^2$). In order for an adequate etch mask (ie one that can survive the duration of the etch process at the feature edge) to be created, a very high dose must be used in order to get a silylation depth that will not be etched away. A back of the envelope calculation illustrates this: it takes nearly 20 nm of silylated resist to form a etch barrier, and during the etch process itself, another 20 nm of silylated resist is consumed, so the feature edge needs to be deprotected and silylated to a depth of 40 nm in order to create an adequate etch mask. This calculation doesn't take into consideration the consequences of the overall contrast that occurs in the 10– 15 mJ / cm² region, or the time to etch the leftover unsilylated resist under the silylated resist, but it demonstrates the point. This was not a problem with PFASO₂ at 193 nm since the energy deposition profile was very deep. This wasn't an issue in the *t*-BOCPS system at 193 nm since the etch rate of the silylated resist was so low (and the etch mask forms with very little thickness loss in *t*-BOCPS).

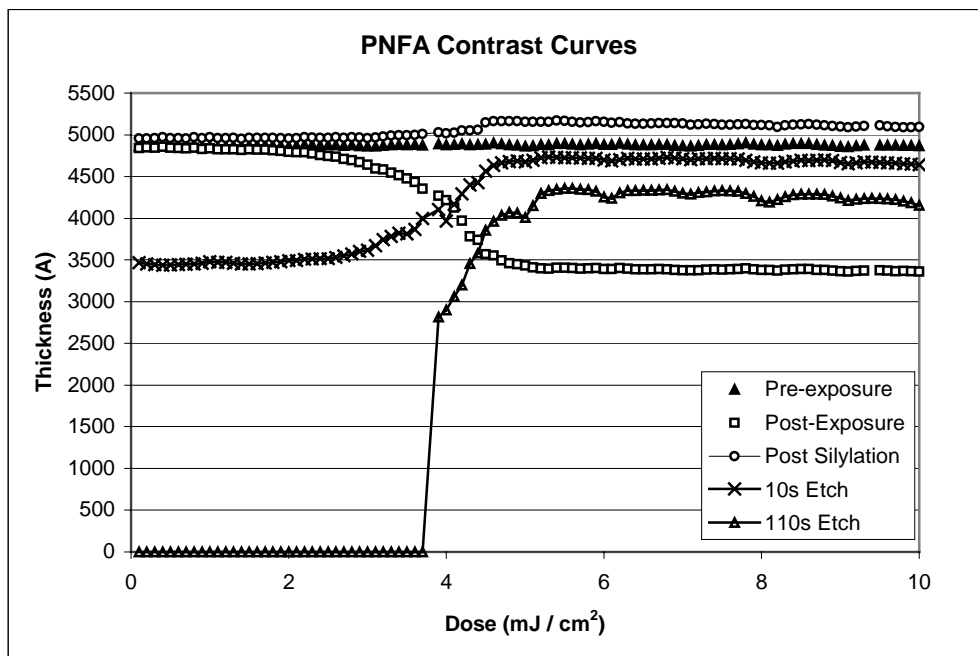


Figure 10. Contrast curves for PNFA

3.2.4 Discussion of contrast curves for PNFA

The deprotection step in PNFA generates sharp contrast at around $4 \text{ mJ} / \text{cm}^2$. The silylation step fills the image in to its original thickness, not enhancing overall system contrast. Finally the etch step enhances contrast, resulting in a sharp overall contrast at around $4 \text{ mJ} / \text{cm}^2$. The slow deprotection step that we saw in the PFASO_2 has vanished by removing the SO_2 from the polymer backbone, and by raising the PEB temperature. The etch rate of this silylated polymer is still relatively high compared to *t*-BOCPS, but the increased transparency and better contrast of the resist drops the imaging dose at 157 nm to a more reasonable level of $\sim 15 \text{ mJ} / \text{cm}^2$ for a binary mask.

4. CONCLUSIONS

TSI is a process that has the potential to overcome many of the challenges facing the lithographic community at 157 nm. It is capable of printing smooth, high aspect ratio, high resolution images that do not suffer feature collapse problems, while using polymers that are substantially more absorbing than those used in single layer applications. Until recently, TSI has had significant line edge roughness problems, but this can be overcome by using polymers that are moderately transparent and have high T_g 's in the silylated state. This paper demonstrates that TSI is capable of printing smooth images at 157 nm, and with proper development, could be a viable imaging alternative to single layer resists.

5. ACKNOWLEDGEMENTS

The authors would like to thank SEMATECH, David Wheeler, Triquest Chemical Company, and AZ Clariant Corporation for their technical contributions to this work. This work was funded by the Semiconductor Research Consortium and DARPA (contract #L-460) and a SRC graduate research fellowship.

6. REFERENCES

-
- ¹ R. R. Kunz, T. M. Bloomstein, D. E. Hardy, R. B. Goodman, D. K. Downs, J.E. Curin, *Proc. SPIE* **3678**, 13 (1999)
 - ² C. Brodsky, *et al*, *J. Vac. Sci. Technol. B*, **18 (6)**, 3396-3401 Nov/Dec (2000)
 - ³ R. J. Hung, *et al*, *Proc. SPIE* **4345** (2001)
 - ⁴ A. P. Mahorowala, *et al*. *SPIE* **4343** (2001)
 - ⁵ J. Cobb, W. Conley, F. Huang, T. Lii, S. Usmani, S. Hector, W. Wu, *Proc. SPIE* **4345**, (2001).
 - ⁶ R. Sooriyakumanaran, D. Fenzel-Alexander, N. Fender, G.M. Wallraff, R.D. Allen, *Proc. SPIE* **4345**, (2001).
 - ⁷ M. H. Somervell, D. S. Fryer, B. Osborn, K. Patterson, C. G. Willson, *J. Vac. Sci. Technol. B* **18(5)**, 2551-2559 Sep/Oct (2000)
 - ⁸ W. D. Domke, V. L. Graffenberg, S. Patel, G. K. Rich, H. B. Cao, P. F. Nealey, *Proc. SPIE* **3999**, 313 (2000)
 - ⁹ S. A. MacDonald, H. Schlosser, N. J. Clecak, C. G. Willson, J. M. J. Fréchet, *Chem. Mater.* **4**, 1364 (1992).
 - ¹⁰ H. Ito, S. A. MacDonald, R.D. Miller, C. G. Willson, *U.S. Patent 4,552,83*, (1985).
 - ¹¹ S. V. Postnikov, M. H. Somervell, C. L. Henderson, C. G. Willson, S. Katz, J. Byers, A. Qin, Q. Lin, *Proc. SPIE* **3333**, 997 (1998).
 - ¹² S. A. MacDonald, H. Schlosser, H. Ito, N. J. Clecak, C. G. Willson, *Chem. Mater.* **3**, 435-442 (1991)
 - ¹³ H. Ito, N. Seehof, R. Sato, T. Nakayama, M.Ueda, *Micro- and Nanopatterning Polymers*, ACS Symposium Series **706**, 210-212